

# Distortion of gamma-ray burst light curves by gravitational microlensing

L. L. R. Williams and R. A. M. J. Wijers

*Institute of Astronomy, Madingley Road, Cambridge, CB3 0HA*

*Email: llrw@ast.cam.ac.uk and ramjw@ast.cam.ac.uk*

Submitted 3 September, 1996

## ABSTRACT

If at cosmological distances, a small fraction of gamma-ray bursts should be multiply imaged by intervening galaxies or clusters, resulting in the appearance of two very similar bursts from the same location with a relative time delay of hours to a year. We show that microlensing by individual stars in the lensing galaxy can smear out the light curves of the multiply imaged bursts on millisecond time scales. Therefore, in deciding whether two bursts are similar enough to qualify as multiple images, one must look at time scales longer than a few tens of milliseconds, since shorter time scales are possibly rendered dissimilar by microlensing.

**Key words:** gamma-ray bursts – gravitational lensing.

## 1 INTRODUCTION

After more than two decades of observations, Gamma-Ray Bursts (GRBs) remain arguably the most puzzling phenomena in astronomy. In particular, their distance scale is yet to be established to everyone's satisfaction, with 100 kpc (Galactic corona) and  $z = 1$  ( $\sim$  few Gpc) being the main opposing candidates (see Fishman 1995). There are two major pieces of evidence that point to the cosmological origin of the GRBs. First, evidence of redshift in faint gamma-ray bursts has emerged, both from time dilation in faint bursts relative to bright ones (Norris et al. 1994, 1995) and from the observation that the peak energies of the spectra are lower for faint bursts (Malozzi et al. 1995), each effect placing the faint bursts at a redshift of about 1. Both effects are only detectable in a statistical sense because the durations and hardnesses of gamma-ray bursts range widely at any given brightness, and subtleties of data analysis therefore play a role, leading others to not detect the time dilation (Mitrofanov et al. 1996). Also, there could be intrinsic correlations between the different properties of a gamma-ray burst that mimic redshift effects, though they are distinguishable in principle from the real thing, and in fact a cosmological origin agrees better with the detected time dilation (see Wijers & Paczyński 1994).

Second, evidence has been found of correlations between bright gamma-ray bursts and objects at their expected redshift (if cosmological) of a few tenths. Recently, Rood & Struble (1996) and Marani et al. (1996) showed that the brighter of the GRBs are correlated with Abell (ACO) clusters. Larson, McLean, and Becklin (1996) found an excess

of galaxies at K band near well-localized gamma-ray bursts. The significance of these is not yet very great, but may improve with time.

It has been pointed out that strong gravitational lensing, resulting in a GRB being split into more than one macroimage, may provide the best means to ascertain the cosmological origin of GRBs (Paczynski 1986b). If a multiply imaged lensing event is observed, then the source can be assumed to be at a cosmological distance from us. How do we know if two bursts originating from the same location, to within the errors, are multiply imaged and are not due to a repeater or are simply two unrelated events? If the observations are free of noise, and microlensing by stars is unimportant, then the multiple images (macroimages) due to an intervening galaxy or cluster should have identical spectra and light curves, to within a scale factor equal to the relative image magnifications. The presence of noise will degrade the light curves, thus macroimages can appear dissimilar. The effect of noise and faintness of the macroimages on their potential classification as 'identical' was discussed by Wambsganss (1993) and Nowak & Grossman (1994). Here we consider microlensing by individual stars in the lensing galaxy, and show that it can 'smear' image light curves on time scales of up to a few tens of milliseconds, making multiple images of the same burst even less similar.

Should one expect to see multiply imaged GRBs if they are at cosmological distances? Mao (1992) and Grossman & Nowak (1994) estimated that the waiting time for one lensed pair to show up in the BATSE catalogue can vary from one to well over ten years, depending on cosmology and other

assumptions, so it is by no means certain that a lensed pair will be found with BATSE.

Microlensing by stars is known to be important for some multiply imaged QSOs, for example, Q2237+0305, the Einstein Cross (Irwin et al. 1989, Houde & Racine 1994), and probably H1413+117, the Clover Leaf (Arnould et al. 1993), PG1115+080 (Vanderriest et al. 1986) and possibly a few more QSOs. Therefore it is expected that macroimages of GRBs will also be affected by microlensing. For concreteness, we examine one particular case that can hypothetically be observed. This case roughly corresponds to the image parameters of a well known lens: Q2237+0305 (Wambsganss et al. 1990). We show what would have been observed if the source here were a GRB instead of a QSO.

Throughout this paper we assume a standard cosmology with  $\Omega = 1$ , and  $H_0 = 75 \text{ km s}^{-1} \text{ Mpc}^{-1}$ .

## 2 EXAMPLES OF MICROLENSED GAMMA-RAY BURSTS

### 2.1 Microlensing calculations

The gravitational potential of the lensing galaxy splits a single background burst into multiple macroimages, whose arrival times can differ by anywhere between a few hours to over a year, and whose angular separation will generally be less than several arcseconds. Because the galaxies are made up of stars, the lensing mass of the galaxy is grainy, and therefore the macroimages are also grainy, i.e. they consist of microimages that have a spatial as well as a temporal distribution. Given the poor angular resolution of gamma-ray telescopes, not only the microimages, but also the macroimages cannot be precisely localized. On the other hand, the temporal resolution of some of the brighter GRBs is very good, of order milliseconds, and so the effects of microlensing are important here: the observed macroimages will appear as a sum of many staggered and scaled versions of the original burst.

To quantify the above description, we first need to specify a macrolensing model, and hence the properties of the macroimages. Given these, we can obtain a temporal profile of a microlensed  $\delta$ -function burst, and later convolve it with an observed GRB light curve to produce an example of a possible microlensed GRB profile.

We start with a macrolensing model of a galaxy, given by a non-singular isothermal sphere, with a core radius (See eq. [8.37] and section 8.1.5 of Schneider et al. 1992 for details). Let us now generate a set of macrolensing parameters reminiscent of the actual observed QSO lens, Q2237+0305. In that case, five images are observed, four of similar magnification, and a demagnified central image. In our case, since the lens model is assumed to be circularly symmetric (for simplicity), only three images will be produced, two images of comparable magnification, and a demagnified third one. Let the galaxy core radius be,  $r_c = 0.36 \text{ kpc}$  ( $\theta_c = 0.5''$ ), and its velocity dispersion,  $\sigma_v = 185 \text{ km/s}$ . The source and lens redshifts are  $z_s = 1.7$ , and  $z_l = 0.04$ , respectively. For a source impact parameter,  $\theta_s = 0.125''$ , three images are formed. The two brighter macroimages have magnifications of 9.86 and 9.31, a separation of  $1.72''$ , and a time delay of

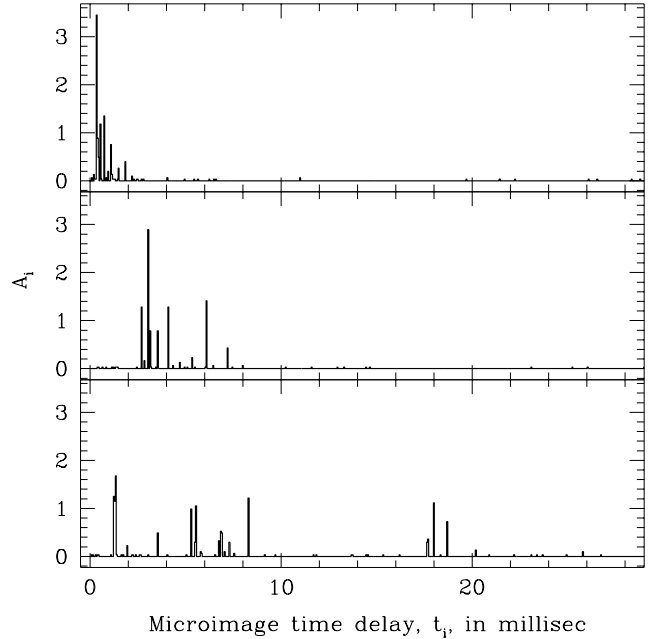


**Figure 1.** Microlensing light curves of a single  $\delta$ -function burst. The macrolensing parameters are  $\kappa=0.524$ ,  $\gamma = 0.354$ , with a total mean magnification of  $\bar{A} = 9.86$ . Horizontal axis is the time delay in milliseconds, and vertical axis is the brightness of individual microimages, such that the total unmagnified brightness of the source is unity. Notice the diversity of microlensing profiles, and that the total time width generally exceeds several milliseconds.

0.92 days. At the locations of these macroimages, the optical depth and shear ( $\kappa$ ,  $\gamma$ ) due to the galaxy are (0.524, 0.354), and (0.799, 0.385), respectively. These parameters are required to generate the microimage distributions.

Given a set of  $\kappa$  and  $\gamma$  for the first of the two macroimages, we can now numerically simulate the action of microlensing on a  $\delta$ -function burst of radiation from a small source. The patch of the lensing galaxy where the macroimage is formed is represented by a two-dimensional random distribution of stars. The mass function of stars is taken from Scalo (1986); it has an average mass of  $\bar{M} = 0.386 M_\odot$ , and an upper and lower mass cutoffs of  $63 M_\odot$  and  $0.087 M_\odot$  respectively. A ray-tracing method implemented using a hierarchical tree code is used to find the microimages of a small source. Once the locations of the microimages are found, the geometrical and gravitational parts of the time delay are calculated for each microimage separately. Figure 1 shows three representative examples of the resulting time series. Note that the three light curves look very different from each other, which is expected since microlensing at even moderate optical depths is a highly non-linear process. A good way to parameterize a given light curve is to calculate its brightness-weighted rms spread  $\Delta t$ ,

$$\Delta t = \sqrt{\frac{\sum_{i=1}^N (t_i - \bar{t})^2 A_i}{\sum_{i=1}^N A_i}}, \quad \text{where} \quad \bar{t} = \frac{\sum_{i=1}^N t_i A_i}{\sum_{i=1}^N A_i},$$

$N$  is the total number of microimages in the lightcurve;  $t_i$ 's and  $A_i$ 's are their individual arrival times and magnifications, respectively. It is evident from Figure 1 that the values of  $\Delta t$  can vary appreciably, even for a fixed set of ( $\kappa$ ,  $\gamma$ ).

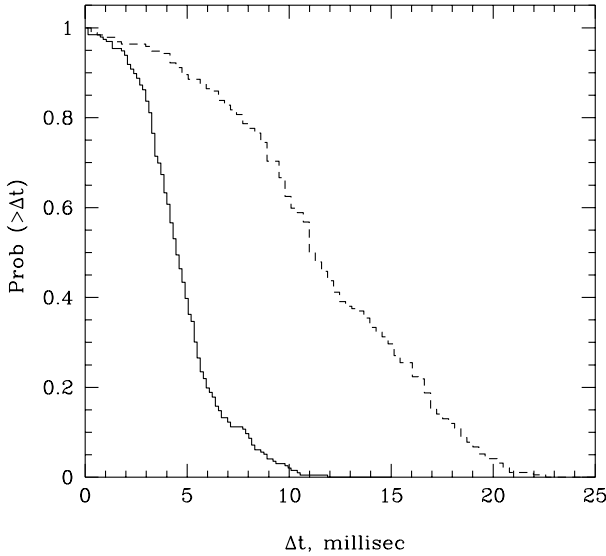


**Figure 2.** Normalized cumulative histograms of time delay spread of microimages,  $\Delta t$  in milliseconds, for a set macroimages with  $\kappa=0.799$ ,  $\gamma = 0.385$  (solid line), and  $\kappa=0.524$ ,  $\gamma = 0.354$  (dashed line).

Figure 2 is a normalized cumulative histogram of  $\Delta t$  values for many independent macroimages having the same  $\kappa$ ,  $\gamma$  values: the solid line is for (0.799, 0.385), and the dashed one for (0.524, 0.354). The median  $\Delta t$  is 5–10 milliseconds, and is therefore relevant for some GRBs.

## 2.2 Application to real GRB light curves

The magnitude and detectability of microlensing distortions depend both on the temporal structure and signal strength of the original burst. To illustrate this, we convolve two of the three microlensing patterns of Figure 1 with two rather different bursts. For this purpose we constructed two time series that after binning and addition of appropriate amounts of noise passably resemble BATSE bursts 1B 910711 and 1B 920218B (the latter shortened by a factor 4 in time). The former was one of the shortest ever seen and contained a sub-millisecond spike (Bhat et al. 1992); the latter is more typical. Figure 3 shows a convolution of microlensing time profiles with the two simulated GRB light curves. As can be seen, the short burst can be distorted beyond recognition, so it would take some courage to advance the view that they are a lensed pair (the paucity of such short bursts would help, of course). The second case is more promising, for its high signal to noise ratio allows one to both recognize the overall similarity at most time scales and the differences at the shortest ones (especially the width of the last spike). From a visual inspection of the first BATSE catalogue (Fishman et al. 1994) it appears that some 20 bursts have visible structure at time scales of 10 ms or shorter, out of 40–50 in which the plot allows one to identify such structure, so the fraction of bursts in which signs of microlensing could be detected if they were a member of a lensed pair may be as high as 50%.

## 3 TIME WIDTH OF THE MICROIMAGE DISTRIBUTION

It is interesting to note that the temporal extent of microimages (Figure 1) is much larger than the time delay between two images created by a single isolated star. In the latter case, time delay is approximately  $8GM/c^3$ , which is about 0.04 ms for a solar mass star-lens if the images are of comparable brightness. This difference between the time width of microimages in a galaxy and those due to an isolated star occurs because a collection of stars, as in a galaxy, act together to produce a wider  $\Delta t$  than a single isolated star.

Before we proceed to derive a rough analytic expression for the total time spread of a microlensed burst, we note that our analysis is related to that of Katz, Balbus & Paczyński (1986). However, there is a difference between the two approaches that makes Katz et al. result not directly applicable to our case. Just like we do below, Katz et al. look at the distribution of microimage magnifications. They pose a question, “What is the size of the region in the lens plane that catches a given percentage of the macroimage flux?”. Below, we answer a somewhat different question, “At what distance from the source does the magnification of individual microimages become a certain fraction of the macroimage flux?”.

Imagine a two-dimensional star field of microlenses of optical depth  $\kappa$ , and let all stars have the same mass of one mass unit. Consider a background source whose unperturbed position coincides with the centre of the coordinate system. Roughly, there will be at least  $N + 1$  images formed: a primary image, and one image associated with every star-microlens in the vicinity of the source. In other words, the macroimage will consist of a ‘cloud’ of microimages surrounding the unperturbed source position. (For a pictorial representation of a microlensing ‘cloud’ see Paczyński 1986a, and Wambsganss 1990). The size of the cloud is directly related to the geometrical time delay of the microimages. Since the gravitational and geometrical parts of the time delay are of the same order, one simply needs to know the size of the cloud in order to estimate the total time delay of microimages. We will now calculate the radius of this cloud.

Consider a microlens on the  $x$ -axis, a distance  $L$  from the origin, where  $L$  is large compared to the Einstein ring radius of a microlens. An image due to this microlens will be located at  $x = L + x'$ , where  $x'$  is small. There are two contributions to the deflection angle in this case: the microlens itself, and a sheet of microlenses interior to  $L$ . On average, the mass of this sheet is  $\kappa L^2$ . The total deflection angle is then given by  $\alpha_x = \kappa L^2/x + 1/x'$ , and  $\alpha_y = 0$ . The magnification of the microimage,  $A^{-1} = 1 - \gamma_\star^2$ , is due to shear only\*, since by assumption there is no continuously distributed matter. The shear is given by  $\gamma_\star = \kappa - x'^{-2} \sim x'^{-2}$ . Solving the lensing equation,  $0 = x - \kappa L^2/x - 1/x'$ , for the location of the images, one finds that  $1/x' \sim (1 - \kappa)L$ . Therefore, we arrive at the following relation between the source-microlens separation and the magnification of the corresponding microimage,  $L^4 \sim A^{-1}(1 - \kappa)^{-4}$ .

So far we have assumed external shear to be 0, there-

\* Note that this shear,  $\gamma_\star$ , is different from the external shear,  $\gamma$ . The latter is due to the overall potential of the galaxy, while the former is due to the matter distribution close to the macroimage.

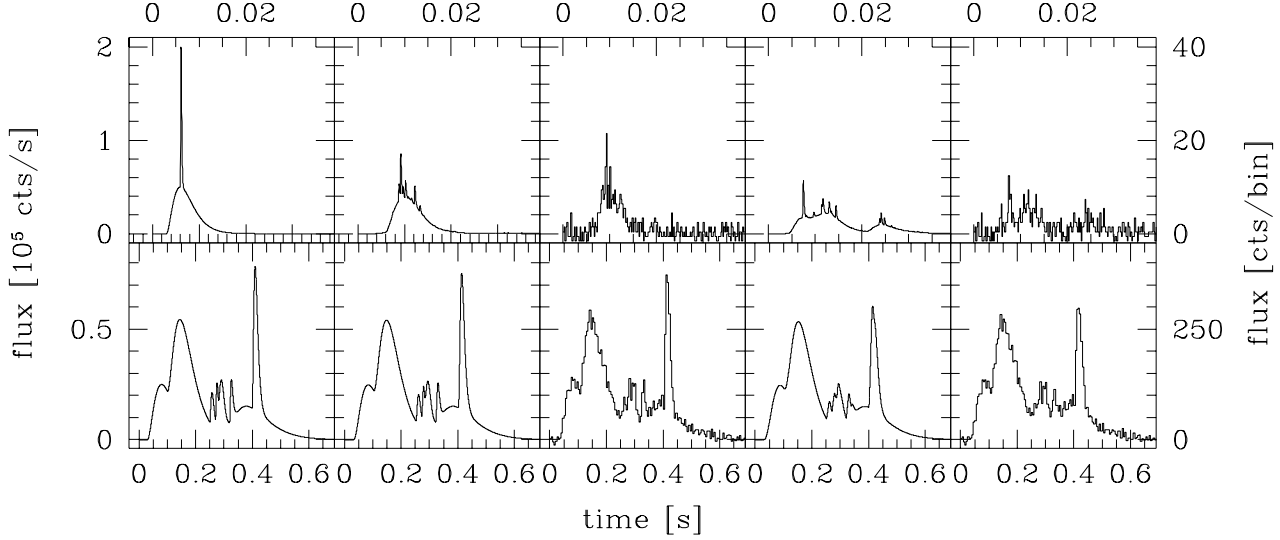


**Figure 3.** A short (top row) and long (bottom row) synthetic gamma-ray burst affected by microlensing. The leftmost panel shows the ideal burst. The next two panels show how it is changed by folding the ideal GRB with the top microlensing pattern of Figure 1, before and after binning and adding realistic noise. The next panels are the same for folding with the bottom microlensing pattern of Figure 1.

fore the distribution of microimages is circularly symmetric with the diameter proportional to  $(1 - \kappa)^{-1}$ . If external shear is introduced, the overall shape of the microimage cloud will get elongated, with the major and minor axes proportional to  $(1 - \kappa - \gamma)^{-1}$  and  $(1 - \kappa + \gamma)^{-1}$  respectively<sup>†</sup>. Since it is the longer of the axes that determines the total width of microimage distribution, the final expression is,  $L^4 \sim A^{-1}(1 - \kappa - \gamma)^{-4}$ .

The total width of the arrival times of various microimages is roughly the time delay of the outermost microimage of sufficiently non-small  $A$ . In our dimensionless units, a single isolated microlens will produce a time delay of 1 between microimages of comparable brightness. By comparison, a sheet of microlenses will have a width of time delays of  $L^2 \sim A^{-1/2}(1 - \kappa - \gamma)^{-2}$ . For example, if images as faint as 0.01 times the source brightness are considered, i.e.  $A = 0.01$ , and  $\kappa = 0.524$ , and  $\gamma = 0.354$  (as before) the total temporal extent of microimages is 671 dimensionless units, or, accounting for the  $\bar{M}$  and  $(1 + z_l)$  time dilation factor, about 10.8 milliseconds.

The straight line in Figure 4 is the analytical derivation presented above. The points are the results of our numerical simulations using the ray-tracing code. The y-coordinate of each point,  $\langle \Delta t \rangle$ , is the average of  $\Delta t$ , as defined at the end of Section 2.1, over many realizations of the source position. A range of  $\kappa$ ,  $\gamma$  parameters were used to test the analytical formula. The fit seems to be good considering the simplicity of our derivation.

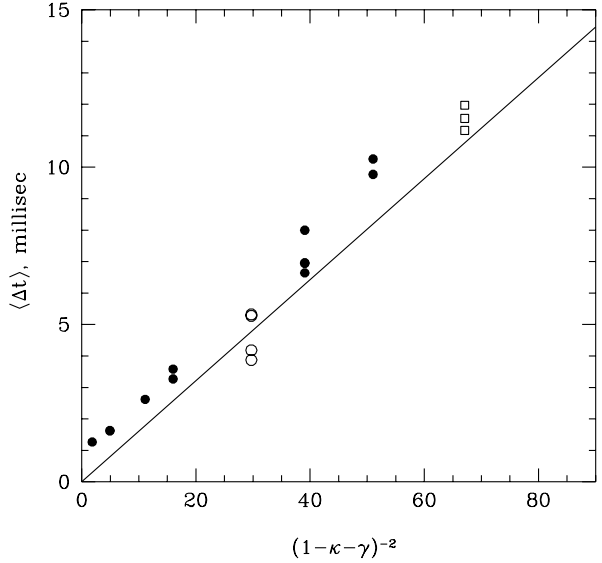


**Figure 4.** Analytically-derived (straight line, see Section 3) and numerically calculated (points) relation between the rms spread of microlensing delays and the macrolensing quantity,  $(1 - \kappa - \gamma)^{-2}$ . Empty circles and squares correspond to the  $(\kappa, \gamma)$  cases represented by solid and dashed histograms, respectively, in Figure 2. The straight line is,  $\langle \Delta t \rangle = (1 + z_l) (8GM/c^3) \bar{M} A^{-1/2} (1 - \kappa - \gamma)^{-2}$ , where  $z_l = 0.04$  (reminiscent of the 2237+0305 quadruple QSO lens),  $A = 0.01$  (see text), and  $\bar{M} = 0.386M_\odot$ .

#### 4 GRB OBSERVABLES AND MICROLENSING

In general, all macroimages of a multiply images GRB will be affected by microlensing to some degree, since the quantity  $(1 - \kappa - \gamma)^{-2}$  of macroimages is usually greater than a few.

<sup>†</sup> This is valid if  $\kappa < 1$ . If  $\kappa > 1$ , the major and minor axes are proportional to  $(1 - \kappa + \gamma)^{-1}$  and  $(1 - \kappa - \gamma)^{-1}$ .

However what one really wants to know, when faced with a pair of candidate macrolensing events, is how much that particular pair has been affected. We will now show that there is insufficient information in the two gamma-ray bursts to estimate this independently.

A macroimage is strongly affected by microlensing if the temporal extent of microimages is sufficiently large. The parameter that determines the temporal spread of the microimages is  $(1 - \kappa - \gamma)^{-2}$ . Therefore, one would want to know this quantity for each of the images.

Given a pair of suspected macroimages, two parameters can be observed: the ratio of the total fluxes of the GRBs, which is roughly the magnification ratio of the two macroimages,  $A_1/A_2$ , and their relative arrival time,  $\Delta T$ . The filled dot on the left panel of Figure 5 is an example of such a set of observables. The lines correspond to  $\log(A_1/A_2)$  vs. dimensionless  $\Delta T$  of the brighter of the two images produced by a non-singular isothermal (solid lines), and a de Vaucouleurs (dashed lines) lens model. The two lines of each model have different central mass densities; since the identity of the galaxy lens will not be known in such cases, its central mass density will be unknown to within a factor of 2–3. The four dots on the right panel of Figure 5 show the corresponding  $(1 - \kappa - \gamma)^{-1}$  values of the primary image, in these four models. It is seen that a set of  $A_1/A_2$  and  $\Delta T$  does not constrain the  $(1 - \kappa - \gamma)^{-1}$  of the macroimage.

To make things worse, there is uncertainty in the values of  $A_1/A_2$  and  $\Delta T$ . The ratio of magnifications can be affected by microlensing, realistically, by up to a factor of 2, or 0.3 in the log. The relative time delay is uncertain because it is proportional to  $(D_{os}/D_{ol}D_{ls})r_0^2$ , where  $D$ 's are the angular diameter distances between the source, lens and observer, and  $r_0$  is the length scale appropriate to the macrolens model: core radius for the isothermal model, and effective radius for the de Vaucouleurs model. For realistic ranges of GRB source redshifts, 0.8–1.2, and lens redshift, 0.2–0.4, there is a 30–50% uncertainty in the cosmological parameter value; and a factor of at least 2 uncertainty in the core/effective radius. Thus there is a factor of at least 4–5 uncertainty in the value of  $\Delta T$ , and our lack of knowledge about the particulars of the lensing galaxy makes the determination of  $(1 - \kappa - \gamma)^{-1}$  virtually impossible.

Finally,  $(1 - \kappa - \gamma)^{-1}$  is related to the *average* of  $\Delta t$ 's; in any particular case,  $\Delta t$  can assume a range of values, even if  $(1 - \kappa - \gamma)^{-1}$  is known precisely (see Figures 1 and 2).

## 5 SUMMARY

It has already been pointed out (Wambsganss 1993) that macrolensed copies of a single GRB need not look alike due to noise, and faintness. In this paper we discuss another reason: microlensing due to stars in the lensing galaxy. Most of the models of GRBs predict the ‘emitting region’ to be much smaller than the Einstein ring radii of even the smallest lenses. The former is of the order of  $10^{13}$  cm, while the latter is roughly  $10^{14}$  cm for a  $10^{-5}M_\odot$  compact object. The microlensing light curve of a short flash originating from a compact region is a series of spikes; the spikes are due to individual microimages, each with a different arrival time. The width of their time distribution is a function of the optical depth and shear of the galaxy at the location of the

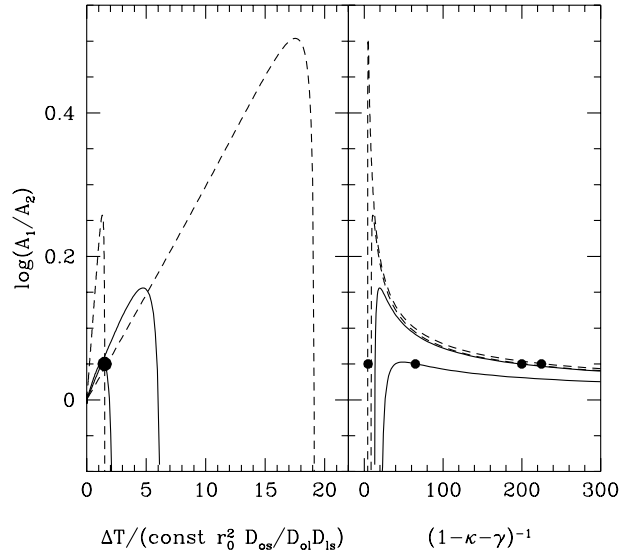


**Figure 5.** Relative macroimage magnifications,  $\log(A_1/A_2)$ , vs. relative time delay,  $\Delta T$ , and  $(1 - \kappa - \gamma)^{-1}$  of the primary image. Four macrolens models are considered: two non-singular isothermal spheres, and two de Vaucouleurs profiles, each with a different, but realistic, central surface mass densities. Notice that a single set of  $\log(A_1/A_2)$  and  $\Delta T$  (large dot on the left panel) can correspond to four very different  $(1 - \kappa - \gamma)^{-1}$  (four dots on the right panel). This example demonstrates that GRB observables are insufficient to determine the extent to which macroimages have been affected by microlensing.

macroimages, and is 5–10 milliseconds for typical values of  $(\kappa, \gamma)$  of the lensing galaxy, and a typical stellar mass function, with an average mass of a few tenths of  $M_\odot$ . Therefore GRB light curves are expected to be affected on these time scales. Similarly, if GRB spectra are varying on these time scales, they too will be affected.

## ACKNOWLEDGMENTS

We would like to thank Andrew Lyne for a lively discussion that inspired this work, and Martin Rees for useful discussions. We acknowledge the support of PPARC fellowships at the Institute of Astronomy, Cambridge.

## REFERENCES

- Arnould, P., et al., 1993, in Proc. of the 31st Liege Intl. Colloq., eds. J. Surdej, D. Fraipont-Caro, E. Gosset, S. Refsdal, M. Remy
- Bhat, P.N., Fishman, G.J., Meegan, C.A., Wilson, R.B., Brock, M.N., & Paciesas, W.S., 1992, Nat, 359, 217
- Fishman, G.J., 1995, PASP, 107, 1131
- Fishman, G.J., et al., 1994, ApJS, 92, 229
- Grossman, S.A., & Nowak, M.A., 1994, ApJ, 435, 548
- Houde, M., & Racine, R., 1994, AJ, 107, 466
- Irwin, M.J., Webster, R.L., Hewett, P.C., Corrigan, R.T., Jedrzejewski, R.I., 1989, AJ, 98, 1989
- Katz, N., Balbus, S., & Paczyński, B., 1986, ApJ, 306, 2
- Larson, S.B., McLean, I.S., & Becklin, E.E., 1996, ApJ, 460, L95

- Malozzi, R.S., Paciesas, W.S., Pendleton, G.S., Briggs, M.S., Preece, R.D., Meegan, C.A., & Fishman, G.J., 1995, *ApJ*, 454, 597
- Mao, S, 1992, *ApJ*, 389, L41
- Marani, G.F., Nemiroff, R.J., Bonnell J.T., & Norris, J.P., 1996, *astro-ph/9607158*
- Mitrofanov, I.G., Chernenko, A.M., Pozanenko, A.S., Briggs, M.S., Paciesas, W.S., Fishman, G.J., Meegan, C.A., Sagdeev, R.Z., 1996, *ApJ*, 459, 570
- Norris, J.P., Bonnell, J.T., Nemiroff, R.J., Scargle, J.D., Kouveliotou, C., Paciesas, W.S., Meegan, C.A., & Fishman, G.J., 1995, *ApJ*, 439, 542
- Norris, J.P., Nemiroff, R.J., Scargle, J.D., Kouveliotou, C., Fishman, G.J., Meegan, C.A., Paciesas, W.S., & Bonnell, J.T., 1994, *ApJ*, 424, 540
- Nowak, M.A., & Grossman, S.A., 1994, *ApJ*, 435, 557
- Paczyński, B., 1986a, *ApJ*, 301, 503
- Paczyński, B., 1986b, *ApJ*, 308, L43
- Rood, H. & Struble, M., 1996, *MNRAS*, submitted
- Scalo, J., 1986, *Fund. of Cosmic Physics*, 11, 1
- Schneider, P., Ehlers, J., & Falco, E.E., 1992, *Gravitational Lenses*, Springer-Verlag Press
- Vanderriest, C., Wlérick, G., Lelièvre, G., Schneider, J., Sol, H., Horville, D., Renard, L., & Servan, B., 1986, *A&A*, 158, L5
- Wambsganss, J., 1993, *ApJ*, 406, 29
- Wambsganss, J., 1990, Ph.D. Thesis, MPA report 550
- Wambsganss, J., Paczyński, B., & Schneider, P., 1990, *ApJ* 358, L33
- Wijers, R.A.M.J., & Paczyński, B., 1994, *ApJ*, 437, L107